

# Incorporating field wind data into FIRETEC simulations of the International Crown Fire Modeling Experiment (ICFME): preliminary lessons learned

Rodman Linn, Kerry Anderson, Judith Winterkamp, Alyssa Brooks, Michael Wotton, Jean-Luc Dupuy, François Pimont, and Carleton Edminster

**Abstract:** Field experiments are one way to develop or validate wildland fire-behavior models. It is important to consider the implications of assumptions relating to the locality of measurements with respect to the fire, the temporal frequency of the measured data, and the changes to local winds that might be caused by the experimental configuration. Twenty FIRETEC simulations of International Crown Fire Modeling Experiment (ICFME) plot 1 and plot 6 fires were performed using horizontally homogenized fuels. These simulations enable exploration of the sensitivity of model results to specific aspects of the interpretation and use of the locally measured wind data from this experiment. By shifting ignition times with respect to dynamic measured tower wind data by up to 2 min, FIRETEC simulations are used to examine possible ramifications of treating the measured tower winds as if they were precisely the same as those present at the location of the fire, as well as possible implications of temporal averaging of winds or undersampling. Model results suggest that careful consideration should be paid to the relative time scales of the wind fluctuations, duration of the fires, and data collection rates when using experimentally derived winds as inputs for fire models.

**Résumé :** L'expérimentation sur le terrain est une façon de développer ou de valider les modèles de comportement des feux de forêt. Il est important de tenir compte des répercussions des hypothèses reliées à l'endroit où les mesures sont prises au sujet du feu, à la fréquence temporelle des données qui sont mesurées et aux perturbations des vents locaux qui pourraient être dues au dispositif expérimental. Vingt simulations FIRETEC des feux dans les parcelles 1 et 6 de l'Expérience internationale de modélisation des feux de cimes (EIMFC) ont été réalisées en utilisant des combustibles horizontalement homogènes. Ces simulations ont permis d'explorer la sensibilité des résultats du modèle à des aspects spécifiques de l'interprétation et de l'utilisation des données de vent mesurées localement dans cette expérience. En décalant jusqu'à deux minutes les temps d'allumage en ce qui a trait aux données de vent mesurées de façon dynamique dans une tour, les simulations FIRETEC sont utilisées pour étudier les ramifications potentielles reliées au fait de traiter les vents mesurés dans une tour comme s'ils étaient exactement les mêmes que ceux qui sont présents à l'endroit où survient le feu, ainsi que les implications potentielles de faire la moyenne des vents dans le temps ou de sous-échantillonner. Les résultats du modèle indiquent qu'on devrait accorder une attention particulière aux échelles relatives de temps des fluctuations du vent, à la durée des feux et aux taux de collecte des données lorsqu'on utilise des vents expérimentalement dérivés comme intrant pour la modélisation des feux.

[Traduit par la Rédaction]

## Introduction

Between 1995 and 2001, the International Crown Fire Modeling Experiment (ICFME) was carried out in the Northwest Territories of Canada. A large number of experimental

measurements were taken, many of which have been published in various venues such as the Canadian Journal of Forest Research, Special Issue on the International Crown Fire Modeling Experiment (Butler et al. 2004a, 2004b; Cohen 2004; de Groot et al. 2004; Lynch et al. 2004; Payne et al.

Received 21 November 2011. Accepted 13 February 2012. Published at [www.nrcresearchpress.com/cjfr](http://www.nrcresearchpress.com/cjfr) on 12 April 2012.

**R. Linn, J. Winterkamp, and A. Brooks.** Earth and Environmental Sciences Division, Los Alamos National Laboratory, Los Alamos, NM 87545, USA.

**K. Anderson.** Natural Resources Canada, Canadian Forest Service, Northern Forestry Centre, 5320 122 Street, Edmonton, AB T5N 2C5, Canada.

**M. Wotton.** Natural Resources Canada, Canadian Forest Service, Faculty of Forestry, University of Toronto, Toronto, ON M5S 3B3, Canada.

**J.-L. Dupuy and F. Pimont.** INRA (Institut National pour la Recherche Agronomique), Unité de Recherches Forestières Méditerranéennes, Equipe de Prévention des Incendies de Forêt, UR629, F-84914, Avignon, France.

**C. Edminster.** USDA Forest Service, Rocky Mountain Research Station, Flagstaff, AZ 86001, USA.

**Corresponding author:** Rodman Linn (e-mail: [rrl@lanl.gov](mailto:rrl@lanl.gov)).

2004; Putnam and Butler 2004; Stocks et al. 2004a, 2004b; Taylor et al. 2004), and also Alexander et al. (2004). These measurements include wind speed and direction at various locations and time intervals, fuel characteristics within the 10 plots, and a variety of in situ measurements to gauge fire behavior. One objective of a modeling experiment such as the ICFME might be to collect data for the development or calibration of empirical fire models. Another modeling-related use of such an experiment might be to validate physically based or theoretical models or to improve these models through identification of shortcomings. Various modeling exercises have been performed for the fires at ICFME (Butler et al. 2004b; Clark et al. 1999; Linn et al. 2005a). One of the primary reasons for these modeling exercises has been model validation. In a few cases, the simulations also suggest the potential of using models for interpretation of experimental data and offering insight into the events that lead to specific aspects of fire behavior.

Whether models are being developed based on experimental data or simulations are being compared with experiments for validation purposes, the data must be interpreted and melded for use as model input parameters. Fire-behavior models produce predictions of various characteristics of an evolving fire based on a set of initial and boundary conditions. No matter how simple or complex the model is, there are either explicit or assumed conditions that establish the state of the fire and its environment at some known time, as well as the way its environment evolves with time. When a model does not accept or require these types of information explicitly, there are implicit assumptions being made concerning the evolution of the environment surrounding the fire. For instance, if a model does not require information about the evolution of the ambient winds, then implicitly they are assumed to be static or have some fixed pattern.

Various types of models accept data in different forms and with different levels of detail. The amount of detail in the output from these models is generally proportional to the amount of detail accepted as input by the model. Much of the fire-behavior modeling that has been performed for comparison with the ICFME fires involved empirically or physically based point-functional models (Butler et al. 2004b; Cruz et al. 2003, 2004; Linn et al. 2005a), but some of the postexperiment modeling utilized more computationally intensive computational fluid dynamics (CFD) based fire-behavior research models such as the National Institute of Standards and Technology's Wildland-Urban Fire Models (WFDS) and FIRETEC (Clark et al. 1996; Linn et al. 2005a; Mell et al. 2007). There is no universal agreement as to the level of detail that must be accounted for in fire-behavior modeling, but this should not be surprising as the applications of fire-behavior models vary from the development of basic prescribed burning prescriptions, to risk assessment, to daily fire growth forecasts, to development and evaluation of fire mitigation strategies, to various research applications such as studying fire behavior or developing simpler and (or) faster-running fire spread models.

The description of the fire environment as initial or boundary conditions for a model can include a variety of traits, subject to model requirements. In general, it will include either assumed or explicitly stated characterizations of the topography, plus fuel (vegetation) and atmospheric conditions in

the vicinity of the fire. The fuel characteristics might include fuel loads, moisture levels, vertical and horizontal distributions, surface area per unit volume, and fuel heat content. The atmospheric characteristics might include wind speed, direction, and shear profile. These characteristics of the flow field can also be combined with any available information regarding wind fluctuations to specify the required three-dimensional (3-D) array of winds. When a model does not require or accept a particular piece of information, there is an implicit assumption about that condition or the model simply neglects any possible impacts of that specific piece of information.

As part of a Canadian Forest Service – Los Alamos National Laboratory – USDA Forest Service collaborative effort focused on exploring the capabilities and limitations of models such as FIRETEC, a series of FIRETEC simulations of selected ICFME plots was initiated. At the onset of this collaboration, the purpose of these simulations was the identification of any shortcomings of the model, as well as an examination of the possible interactions between the fire, atmospheric flows, fuel structure, and geometrical configuration of the experimental plots. As part of this study, wind and vegetation measurements have been used to generate input data for FIRETEC. At the time of the initial series of FIRETEC simulations, it became apparent that it was essential to do a preliminary investigation regarding a set of issues that must be considered to frame our interpretation of the model results.

In the translation of measured wind data to the 3-D model-input fields, assumptions and approximations must be made. For example, the winds were collected at one location within a cleared area among the set of burn plots. The following questions arise immediately with respect to the use of these data. How do the winds within the cleared areas relate to the winds over or through the vegetated areas? How much spatial and temporal variation is there between the winds at the location where the data are collected and the winds at the site of the fire? What is sufficient temporal resolution for wind data? What are the impacts of the fuel breaks on the wind field and subsequent fire behavior?

This paper is intended to provoke discussion and illustrate some of the considerations that must be taken into account when using measured wind data to drive, calibrate, or validate fire models. This topic is vast, and this paper certainly does not do an exhaustive inventory. However, the intent is to raise awareness and spark discussion on the part of both experimentalists and modelers. These discussions would likely have relevance to the design of future experiments, as well as to those involved in comparing fire models with experiments or developing new fire models. This paper focuses on the use of wind data by the models, but that is not intended to minimize the importance of similar issues regarding the representation of vegetation, which is, in fact, the topic of separate investigations. Although the results of the simulations in this paper agree well with the data, that is likewise not the focal point of this paper.

The following sections include a brief description of the ICFME experiment, the basic capabilities of the FIRETEC model, a method for melding ICFME tower wind data into initial and boundary conditions for FIRETEC, the 20 simulations that were performed for this manuscript, and then a

mention of the relevance and interpretation of the results. The main message and highlights are restated in the conclusions in hopes of sparking discussion within the fire community.

## ICFME overview

The International Crown Fire Modeling Experiment (ICFME) was conducted between the years of 1995 and 2001. Planning for the experiment began in 1994 and included over 100 people from 14 countries and 30 organizations such as the Canadian Forest Service, the US Forest Service, the International Boreal Forest Research Association (IBFRA) Fire working group, and Russia (Stocks et al. 2004a). The intent of the experiment was to help develop a better understanding of, as well as a model for, crown fire behavior utilizing modern instrumentation (Stocks et al. 2004a).

The burns were carried out in the Northwest Territories of Canada near Fort Providence and the junction of the Great Slave Lake and the Mackenzie River (Stocks et al. 2004a). Of the 10 primary plots, eight (named plots 1–8) were approximately 150 m × 150 m. Plot 9 was approximately 100 m × 100 m, and plot A was roughly 75 m × 75 m (Stocks et al. 2004b). Each plot was surrounded by a fuel break approximately 50 m wide and was created by bulldozing and removing the fuel in the break area, leaving nearly bare earth. Vegetation in the plots was primarily composed of jack pine (*Pinus banksiana* Lamb.) overstory with an average height of approximately 12 m and black spruce (*Picea mariana* (Mill.) B.S.P.) understory with an average height of 5.5 m (Alexander et al. 2004). Figure 1 illustrates the layout of the various experimental plots with respect to one another and with respect to the experimental site boundaries. This horizontal arrangement of the plots has been presented in numerous previous reports and publications (Alexander et al. 2004; Stocks et al. 2004a, 2004b). It is included here because various aspects of the layout are very pertinent to later discussions. For the purposes of this paper, the positive  $x$  and  $y$  directions, which are labeled on Fig. 1, are nominally toward the east and north, respectively.

The plots were lit using a fire-line type ignition. A pressurized flame thrower, also known as a “terra torch”, was mounted on a truck and driven along the edge of the plot, perpendicular to the wind (Stocks et al. 2004b). The igniter was aimed at the ground and sprayed a stream of gelled gasoline along the ignition line that was approximately 1 m wide (Taylor et al. 2004). The goal of this ignition method was to try to get fire immediately into the crowns of the plot. Ignition took approximately 60 s for the plots that measured roughly 150 m per side (Stocks et al. 2004b).

## Model description

### FIRETEC

In this section, we first provide a brief overview of the FIRETEC model. However, because FIRETEC performance is not the focus of this paper and detailed descriptions of the physical and chemical formulations of the FIRETEC model have been published previously (Linn 1997; Linn et al. 2002, 2005b; Pimont et al. 2009), they are not presented here. In the second subsection, particular attention is paid to

the input of measured data to the model and related assumptions, implications, and limitations.

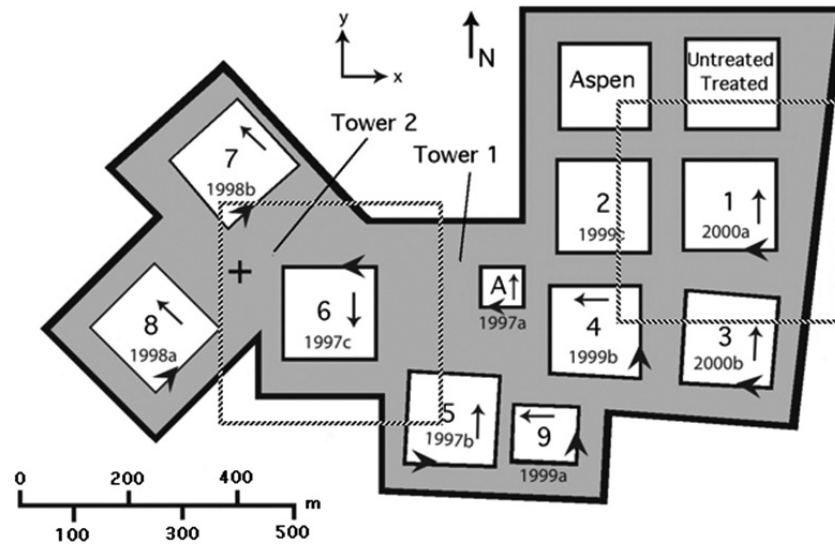
FIRETEC is a 3-D multiphase transport model, based on the ensemble-averaged equations of motion for a compressible fluid, and includes simplified treatments or representations of the combustion and heat transfer occurring in wildland fires. The model uses a multiphase approach to capture the mass, momentum, and energy exchange between the gas and solid phases. Gas properties including various densities, oxygen concentration, potential temperature, mean velocity components, and turbulence quantities are transported and evolved using a set of partial differential equations (transport equations). These transport equations account for processes including reaction rate, convective and radiative heat transfer, vegetation drag, mean flow advection, and turbulent diffusion. The evolution of the fuel moisture and amount of solid fuel that is available for combustion, as well as the heat energy associated with the solid fuel, are computed based on a series of partial differential equations accounting for such processes as evaporation of liquid water and convective and radiative heat transfer to the solid. In this finite volume representation, the fuel and atmospheric properties are resolved in a series of 3-D voxels or computational cells that combine to fill the domain. For the current simulations, various vegetations’ contributions to the fuel matrix are combined to provide a single weighted average for the bulk fuel quantities within each computational cell.

Various approximations and simplifications are built into the FIRETEC formulation for quantities associated with the heterogeneities of vegetation and gas properties within a resolved volume. These simplifications include the use of probability distribution functions to describe temperatures and moisture contents within a resolved volume and transport equations for unresolved turbulence. The reaction rate formulation for the combustion process is based on a mixing-limited assumption and depends on the relative densities of the solid fuel and oxygen, the turbulent diffusion rate, the stoichiometry of the fuel and oxygen, and a probability distribution function for the temperature within a resolved grid volume (for conceptual details, see Linn (1997, pp. 77–79)). The formulation focuses on fine fuels, ignoring solid conduction within the fine fuels and thus assuming that the fuels are thermally thin.

In FIRETEC, the treatment of the turbulent Reynolds stress and the turbulent diffusion coefficient is based on the expectation that more than one important length scale will exist. The turbulence is represented as the sum of three separate turbulence spectra corresponding to two selected near-grid or subgrid sized, fuel structure dependent length scales. The evolution and transport of the Reynolds stress at each scale is then represented in terms of the resolved velocity strain rate and the turbulent kinetic energy associated with each length scale. Linn (1997) contains a more complete description of this treatment of turbulence.

For the ICFME simulations, a Monte Carlo based radiation transport scheme was used to simulate the exchange of photons between the gases, solids, and their environment. The photon sources for this radiation scheme are developed based on probability distribution functions for temperature in the solid and gas phases and a multiphase representation of the unresolved dispersed fine solid vegetation. It should be ac-

**Fig. 1.** Diagram of the ICFME experimental plots, labeled 1–9 and A. Fuel break areas are shaded. The year in which each plot was burned is indicated (letters indicating the sequence within each year), as is the location of the two meteorological towers. The dashed black lines show the horizontal extent of the FIRETEC computational domain for plots 1 and 6. The arrows within the plots indicate the nominal direction of the ambient wind at the time of each of the fires. The arrowhead placed along the side of each experimental plot shows the origin and direction of the ignition line for that plot.



knowledge that the energy absorbed by the large woody mass is heuristically approximated but not allowed to re-emit because the temperatures of these large solids are not tracked.

The governing equations of the combined HIGRAD/FIRETEC model are solved numerically via a conservative forward-in-time technique based on a method of averages (MOA) approach. In this approach, high-frequency waves are treated explicitly in a computationally efficient manner (Reisner et al. 2000). The lateral boundary conditions for these ICFME simulations used a relaxation technique designed to nudge velocities toward presumed ambient velocities at the boundaries. The top of the domain uses a similar relaxation scheme, with the intent of reducing the impact of the top boundary on rising plumes.

#### Assimilating data for initial and boundary conditions

In using FIRETEC to simulate aspects of the ICFME experiment, it was important to remember that no current model is capable of capturing all of the physics that occurs as a part of a wildfire. Therefore, the hope was to capture the gross trends of the observed fire behavior and illustrate a possible set of process interactions and balances that lead to these trends. Simulation of any observed fire requires the collection of adequate fuels and wind data, which often proves to be a significant challenge. Unfortunately, there is a limit to the amount of data collected in any experiment, even ICFME, and usually less is collected for actual wildfire scenarios. Lack of data, lack of data resolution, and (or) data inaccuracy compounds the inherent limitations of physics-based wildfire models such as FIRETEC. In fact, it can be very difficult to differentiate model error from inadequate representation of environmental conditions.

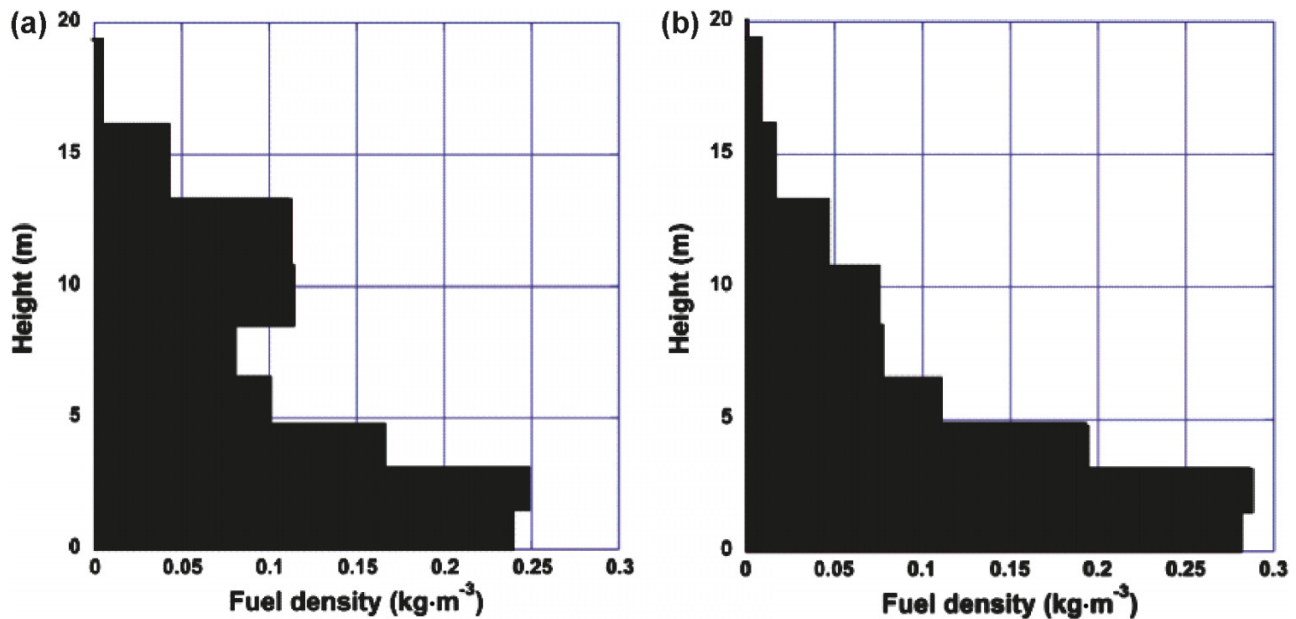
For the simulations included in the present work, the fuel structure within a particular ICFME plot was treated as being laterally homogeneous. The vertical stand structure for each

plot was developed based on information provided in Alexander et al. (2004). Appendix 2 of their document provides the stem diameter-at-breast-height (DBHOB) and height distributions (stems per hectare) of the tree canopy for each of the ICFME plots. Their table 11 provides regression coefficients to predict the crown fuel weight from the DBHOB. Their table 15 provides coefficients to predict the fraction of crown fuel weight from the fraction of tree height. By stepping through the stem data within their appendix, a vertical distribution of fuel load per plot was created. Final fuel densities within each grid cell represent the total fuel loads of needles and roundwood up to 1 cm in diameter, live and dead, for both species. Moisture contents of the fuels were set to values described in Stocks et al. (2004b) and weighted by the fuel load of each component.

In this investigation, we were interested in studying the implications of using observational wind data to drive wildfire simulations. For this purpose, we wanted initially to work with fires that had relatively simple burn patterns and limited fuel heterogeneity to facilitate the identification of the impacts of the wind data. For this reason, as well as the computational cost of doing numerous simulations for each ICFME plot, we chose to focus our attention on plots 1 and 6 in this study. These two particular plots both had relatively continuous spread across the plot, whereas many of the other plots had significant periods of decelerated spread rates or heterogeneities in the fuel. These plots were both 150 m × 150 m, whereas some of the other plots were smaller. In addition, these two plots had two different frequencies of wind data, thus providing a chance to consider the implications of the data-recording strategies.

For the simulations described in this text, the computational domain is 400 m × 400 m horizontally, with a uniform horizontal grid spacing of 2 m. The dashed black lines in Fig. 1 indicate the horizontal extent of the FIRETEC computational domains for plots 1 and 6. The vertical grid spacing

**Fig. 2.** Fuel distributions for (a) plot 1 and (b) plot 6. Each horizontal bar or vertical step indicates the vertical position and dimension of a horizontal layer of computational cells.



is nonuniform, with a value near the ground of approximately 1.5 m increasing to about 30 m at the top of the domain at  $z = 615$  m. Figure 2 illustrates the vertical profiles for the vegetation used in the simulations of plots 1 and 6 of the ICFME. The black lines in these plots represent the total fine fuel density as a function of height. In addition to indicating the fuel density for a column of computational cells for plots 1 and 6, each horizontal bar or vertical step in Fig. 2 indicates the vertical position and dimension of a horizontal layer of computational cells. In other words, the bottom of the step is the bottom of the computational layer, and the top of the step is the top of the computational layer. These black lines compare well with the plots provided in Stocks et al. (2004b), with the realization that the vertical resolution is tighter (1 m) in these previously published diagrams. It is worth noting that the composite vertical fuel profiles for plots 6 and 7 were transposed in the original documents (fig. 12 in Alexander et al. (2004); fig. 3 in Stocks et al. (2004b)). This has been confirmed with the original authors. The vertical distribution of fuel presented in Fig. 2, along with information concerning the horizontal configuration of the ICFME site and experimental plot arrangements, were used to generate 3-D fuel beds for plots 1 and 6.

Figure 3a is a photograph of an oblique overview looking north from outside the ICFME boundary, with plot 9 in the foreground and plots A, 4, 3, 2, and 1 in the background. Figure 3b is a photograph of an overhead oblique view of the northwestern corner of plot 1 as the fire approached the northern side of the plot. The photograph is included to provide the reader with a sense of the scale of the vegetation with respect to the cleared fuel breaks, which are approximately 50 m wide. It also suggests the potential impacts of the vegetation heterogeneity on not only fire behavior (including the intended purpose of the fuel breaks), but also the wind patterns in the immediate vicinity of the plots and in the fuel breaks. Figures 1 and 3 not only illustrate the com-

plexity of the ICFME site, but also show the vast amount of preparation work that must be performed to conduct such an experiment.

The ICFME experimental fires were intended to capture crown fire behavior and so were conducted on days of extreme fire weather. At 61.6°N latitude, the site would experience 19–21 h of sunlight in midsummer, providing significant daytime heating. The average dry-bulb temperature at ignition time for the 10 burns (plots 1–9 and A) was 25 °C, and the average humidity was 35% (Stocks et al. 2004b). Sky conditions were often clear, with high mixing layers (~3000 m on the burning days for plots 1 and 6 based on 00UTC sounding from YSM Fort Smith). Atmospheric stability was considered nearly neutral near the ground and was assumed to be neutral for the height simulated (615 m). This is consistent with the height of the mixing layer, which was approximately 3000 m on both days used in this study (based on the Fort Smith soundings).

Wind measurements were collected at 2, 5, and 10 m on a control tower located in an open area among the plots to be burned that year. The towers collected wind speed and the direction of the horizontal projection of the wind at regular intervals. In 1997, when plot 6 was burned, wind data were sampled every 5 s from tower 2 and then were averaged to 1-min values. For plot 6, only the 1-min averaged data were recorded. In 2000, when plot 1 was burned, wind data were collected once every 5 s from tower 1, and each of these measurements was recorded (Taylor et al. 2004). The location of these towers is shown in Fig. 1. In 1997, it was possible to collect data at higher frequencies; however, at the time, it was thought that 0.0167 Hz (60 s) was more than adequate for these data.

For the ICFME simulations, HIGRAD/FIRETEC uses a time step of 0.02 s. Boundary conditions must be supplied at this frequency, and so a simple smooth fifth-order polynomial curve-fit interpolation scheme was used to estimate the

**Fig. 3.** (a) Overhead oblique view of plot 9 in the foreground and plots A, 4, 3, 2, and 1 in the background prior to the experiment; and (b) photograph of plot 1 as it was burned. Both photographs are courtesy of Natural Resources Canada 2005 ICFME website, with permission from Michael Wotton.

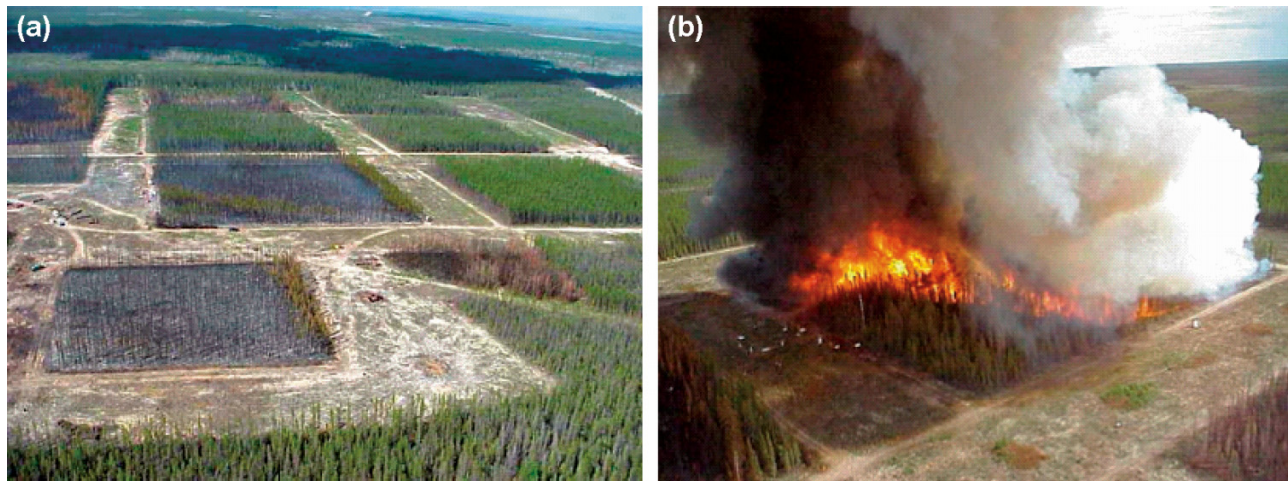
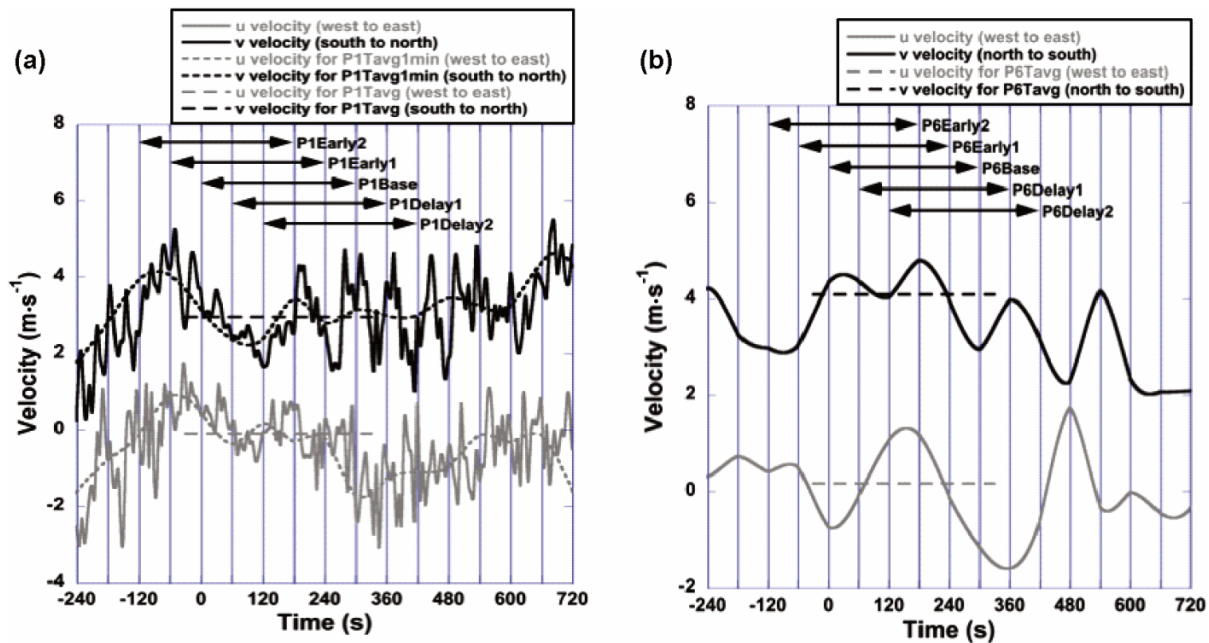


**Fig. 4.** Interpolated  $u$  and  $v$  wind velocity components for (a) plot 1, where data were collected every 5 s, and (b) plot 6, where 1-min average data were collected. Interpolation was performed using a fifth-order polynomial.



evolution of the velocity components between the recorded wind data points. The collected data can easily be transformed into the  $u$ - and  $v$ -velocity components, which are parallel to the  $x$  (or east) and  $y$  (or north) directions, respectively. Figures 4a and 4b illustrate time series plots for  $u$  and  $v$  for 16 min around the time of the burns of plots 1 and 6. The actual burns start at the time designated as 0 s in Figs. 4a and 4b. In Fig. 4, the labeled arrows indicate the window of time when the experimental fires were being carried out. It is clear from the curves in Fig. 4 that the winds were neither constant magnitude nor constant direction when examined at these temporal resolutions. The question arises: Does the frequency of the fluctuations or wind sampling mat-

ter? Another observation concerning these wind fields is that there is not an obvious externally driven shift in the  $u$ -velocity component (the crossstream component, which is pointed towards the experimental plots) during the time of the experiment. The lack of a predominant shift in the winds blowing towards the experimental plots during the fires makes it difficult to determine if the fires were affecting the local winds measured at the towers or not.

The wind measurements at the locations of these two towers contained the most comprehensive description of the evolving wind patterns at the ICFME site at the time of the fires. However, the nature of the resulting data requires extrapolations and assumptions in its interpretation to be used

to specify the ambient winds in a CFD model such as HIGRAD/FIRETEC. CFD models require explicit specification of these data through initial and boundary conditions. The initial conditions for a CFD model are usually specified as a wind velocity vector at every resolved location or in every computational cell within the computational domain. In this case, the domain is a 3-D grid that extends over parts of multiple experimental plots, fuel breaks, and well above the height of the wind control towers.

To specify the initial and boundary conditions for the FIRETEC simulations of the ICFME burns, assumptions were made about how to use the wind data from a tower that was located in a fuel break to suggest the wind conditions elsewhere in the computational domain. There are several factors that complicate the use of the tower data for prescribing initial and boundary conditions. One of the complications is that the towers were in clearings ~100 m from upwind forests, and the data collected from these towers at 2, 5, and 10 m were below the mean height of the surrounding forests (around 12 m). In such an arrangement, the winds at the towers are still affected by the upwind forest, yet they will not have the same profile as exists in or over the forest. Frequently used expressions for estimating vertical profiles such as the logarithmic and power law functions are ideally suited for homogeneous conditions in which the boundary layer has had a chance to adjust to its surroundings and the measured velocities are representative of large areas. Under many wind conditions, this is not the case for these tower measurements due to the spatially heterogeneous arrangements and drastic vegetation discontinuities of the experimental plots and clearing surrounding the towers. For the initial conditions in the clearings, we chose to use a power law wind profile with an exponent of 1/7 (Plate 1971) to extrapolate up from the 10 m measurement. This method was chosen because it has only one degree of freedom. It was difficult to justify the second degree of freedom that exists in the standard log profile in light of the complex situation at the tower likely causing a deviation from any standard extrapolation and the lack of a clearly appropriate second data point or surface roughness suitable for the canopy and clearing. The power law method of estimating wind profiles is commonly used in the wind-energy industry in situations where the surface roughness is not well characterized (Peterson and Hennessey 1978). The horizontal direction of the flow throughout the vertical column was taken to match the 10 m height winds as we did not have evolving information about the directional shear of the winds during the fires.

Another necessary approximation concerns the relationship between the horizontal winds at the tower location and the winds within and above the vegetated experimental plots and site boundaries. For the initial and boundary conditions in clear-cut areas, the vertical profile was defined by the power law as described above. However, in regions where there are trees, the vertical profile would be different. To estimate the initial and boundary conditions in the canopy and to compensate for the fact that the winds inside the canopy would be lower than the winds at the same height in the clearing, we applied a simple linear function that scaled down the local wind speed based on the density of the canopy. This assumption causes the horizontal winds within the vegetated plots to be slower for locations with larger bulk densities. These sim-

ple assumptions were used due to a lack of explicit guidance about the vertical profiles of the wind in this complex experimental site. Equations 1 and 2 show this linear reduction function applied to the power law for the horizontal velocity components in the canopy:

$$[1] \quad u(z) = u_{z=10\text{m}} \left( \frac{z}{10} \right)^{1/7} \left( 1 - \frac{\rho_{f,z=10}}{\rho_0} \right) \beta$$

$$[2] \quad v(z) = v_{z=10\text{m}} \left( \frac{z}{10} \right)^{1/7} \left( 1 - \frac{\rho_{f,z=10}}{\rho_0} \right) \beta$$

where  $z$  is the height above the ground (in metres) and  $u_{z=10\text{m}}$  and  $v_{z=10\text{m}}$  are the measured 10 m tower velocity components from the west and south (plot 1) or west and north (plot 6), respectively.  $\rho_{f,z=10}$  is the density ( $\text{kg}\cdot\text{m}^{-3}$ ) of the fuel at 10 m;  $\rho_0$  is a constant density of  $0.15 \text{ kg}\cdot\text{m}^{-3}$ ; and the constant  $\beta$  equals 0.78 for areas with vegetation that has not been burned previously and 0.45 for plots that have been burned previously (derived from table 3 in Taylor et al. (2004)).

To avoid having an abrupt step in the vertical velocity profiles between the winds in the canopy and the power law wind profile above the canopy, an exponential decay function was applied to the vegetation function such that the effects of the canopy would not stop immediately at the top of the canopy, but would instead taper with height. Equations 3 and 4 illustrate the application of these exponential decay functions for blending the vegetation winds with standard power law winds.

The results of these assumptions are combined in eqs. 3 and 4 below:

$$[3] \quad u(z) = u_{z=10\text{m}} \left( \frac{z}{10} \right)^{1/7} \left( 1 - \frac{\rho_{f,z=10}}{\rho_0} \beta e^{-[\max(0,z-12)/8]} \right)$$

$$[4] \quad v(z) = v_{z=10\text{m}} \left( \frac{z}{10} \right)^{1/7} \left( 1 - \frac{\rho_{f,z=10}}{\rho_0} \beta e^{-[\max(0,z-12)/8]} \right)$$

It can be seen from eqs. 3 and 4 that the “max” function causes the exponential function to have a nonunity value only above the canopy. The linear vegetation impact function has an effect only in vegetated regions (within and above the canopy). The winds over the vegetated plots and over the clearings approach one another quickly with height. These equations are used to specify the initial vertical profile of winds at every  $x,y$  location within the domain, thus filling the domain with estimates of the horizontal winds for initial conditions. Once the simulations start, these profiles adjust to become in balance with the drag of the vegetation and the heterogeneity of the site. To allow the initial conditions to evolve to a more realistic state, the simulations were run for 30 s before the fires were ignited.

Equations 3 and 4 provide the vertical profile of the evolving winds at the inlet boundaries as well. The details of the inlet velocity profiles in the vegetation are quickly modified by the vegetation drag inside the domain. Thus, the main impact of these profiles is to establish the direction and magnitude of the wind near the top of the vegetation at the

boundaries. After a simulation is started, the specified vertical wind profile's only influence is at the edges of the domain because the coupled fire-atmosphere CFD model determines all of the interior velocities.

It is also assumed that the direction of the initial non-fire-influenced winds, as well as those evolving conditions at the boundaries, are in the same direction as those of the measured tower wind data everywhere in the domain. This assumption is based on the fact that there is not sufficient information to suggest, much less specify, the spatial heterogeneity patterns of even the ambient wind fields, much less those influenced by the geometry of the experimental site. It was assumed that the ambient winds evolved simultaneously around the outside of the 400 m × 400 m computational domains. There is some error in this assumption because the flow structures are propagating at some finite speed; however, the spatial scale of the flow structures and the speed at which they are propagating are not known.

Close consideration of this method of specifying initial and boundary conditions reveals that there are sharp horizontal gradients in the velocity fields, even above the vegetation heights, because the vegetation densities are discontinuous at the sides of the plots. Examination of simulation results suggests that these sharp gradients heal themselves quickly with time in the case of the initial conditions and within a few computational cells in the case of the boundary conditions. Due to the lack of data, there are no vertical velocities specified in the initial or boundary conditions, which also forces some quick adjustments by the CFD model to assure conservation of mass and momentum at the edges of the plots.

A simple test was performed to examine the consistency of the boundary and initial conditions with the measured data. For this test, a wind simulation was performed in which the boundary and initial conditions were specified using the methods described, and the winds within the fuel breaks were compared with the measured tower velocity profiles. In this test, the simulated velocity profiles in the breaks were similar to those of the winds measured at the tower at 2, 5, and 10 m heights. This test suggests that although the vertical profiles are not likely to be exactly what was present on site at the time of the burns, these conditions are not incompatible with the tower measurements.

One of the drawbacks of taking data at one isolated tower is that it is very hard to interpret the temporal fluctuations in the wind measurements in terms of spatial heterogeneity in the winds that are advecting past the towers. In other words, with the information available, it is impossible to differentiate small spatial flow structures moving slowly past the tower from large flow structures moving more quickly past the tower.

In each of the simulations performed for this study, the simulation start time was chosen 30 s prior to the desired ignition time to allow the winds to equilibrate across the domain and begin to evolve in response to the dynamic boundary conditions, which were set according to the measured wind data for these preignition times. At the desired time of the ignition, a dynamic heat source was applied to the fuel. This heat source was intended to capture some of the attributes of the dynamic ignition that occurred in the experiments as a truck with an igniter drove from one corner of a plot to another corner, establishing a strong ignition source. In the

simulations, the ignition location covered the 150 m distance from one corner of the plot to another in 1 min, which is the estimated rate at which the ignition line was drawn in the experiments.

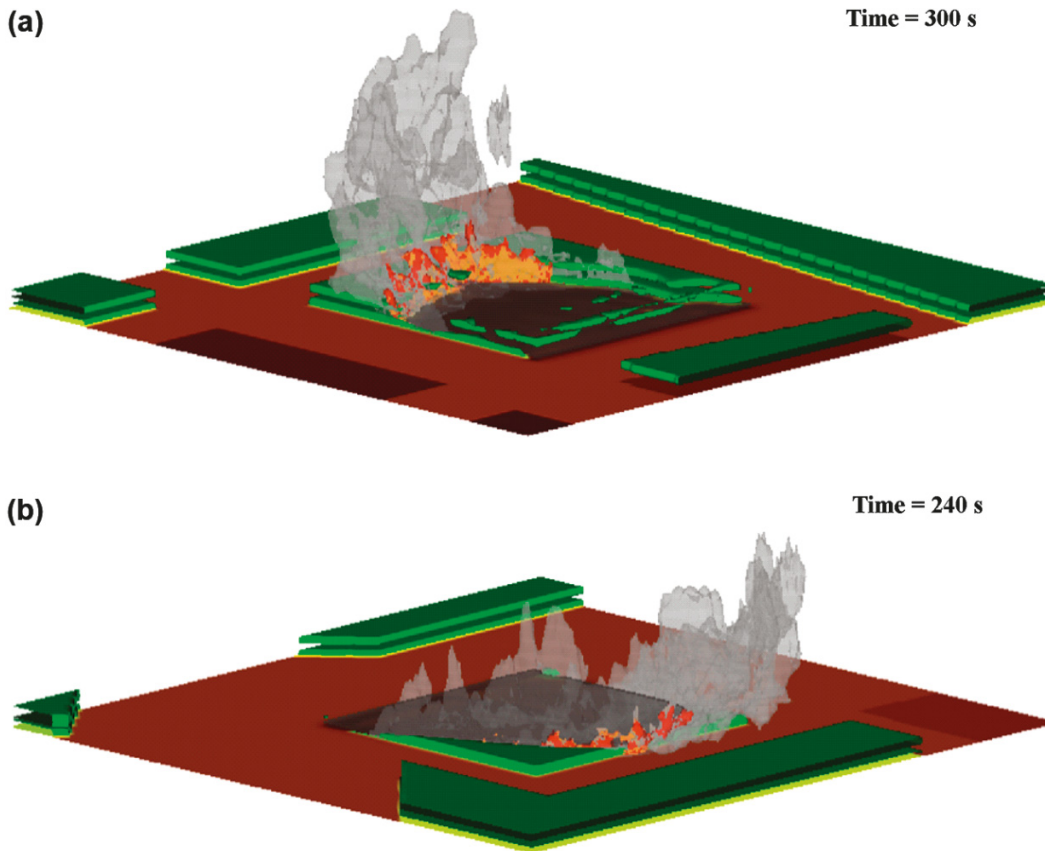
In light of the fact that actual tower measurements are being used to drive the evolution of the ambient winds in the simulation, the natural tendency is to synchronize the wind time series with the reported ignition time in the experiments. In other words, the wind forces at the boundaries of the simulation domain at the time of ignition in the simulation would be those seen at the tower at that same time. However, under closer inspection, this assumption is suspect and could lead to the ignition being out of sync with winds that were likely to exist at the ignition location at the time of the ignition. Unfortunately, because the towers are separated by approximately 600 m crosswind and 150 m downwind from the center of the ignition line for plot 1 and 200 m and 50 m from the center of ignition for plot 6 and there is a finite propagation speed and finite size of the atmospheric flow structures, the fluctuations felt at the tower are not exactly the same as those felt at the ignition line simultaneously. For this study, the assumption is made that the character or nature of the fluctuations at the tower is representative of those at the burn plot; however, it is acknowledged that the phase and details could be different.

## Simulations

For the purpose of this study, simulations of the plot 1 and plot 6 fires were performed using the methods and assumptions discussed above. For all of the simulations described in this study for plot 1, the same homogeneous fuels were specified within the plot, and similarly for the simulations of the plot 6 fire. For each of the plots, a simulation was performed using both the  $u$  and  $v$  components of the dynamic wind field in sync with the ignition of the fire. Because we are using both horizontal components and allowing them to vary with time, the winds are effectively rotating with time and are not held fixed perpendicular to the ignition line. These simulations, referred to as BASE1 and BASE6, are used as reference simulations in the explorations that follow and are shown in Fig. 5. In addition to these base-case simulations, additional simulations were performed for each plot to investigate the implications of the approach, interpretations, simplifications, and assumptions for using the meteorological tower data to drive the fire simulations as described above. These simulations are summarized in Table 1. The results of these simulations suggest an interesting set of considerations for both modelers and experimentalists.

P1Base and P6Base are the most obvious simulations to perform based on the available data and documented time of ignition. However, the scale of the experimental plots, frequency of the variations in the wind data, and location of the towers with respect to the experimental plots suggests a need to explore the implications of phase mismatches between winds at tower locations and the burn plots. In other words, because the fluctuations that strike the tower at the time of the burn are not exactly the same as those that pass over the experimental plot during the fire, it is important to understand how significant these differences might be. A first-order assumption can be made that the general character of the wind fluctuations at the burn plots is similar to that at

**Fig. 5.** (a) P1Base simulation at 300 s after ignition, and (b) P6Base simulation at 240 s after ignition. Both images are viewed from the southwestern corner of the computational grid. Green isosurfaces indicate locations where fuel densities including moisture are greater than  $0.15 \text{ kg}\cdot\text{m}^{-3}$ . Orange, red, and grey isosurfaces indicate locations of hot gas emissions.



the tower, and thus possible wind sequences at the location of the fire can be obtained by shifting the phase of the ignition with respect to the winds. By initiating the simulated ignitions 120 s or 60 s early or 60 s or 120 s late, it is possible to explore potential implications of the specific phase of the wind fluctuations on the experimental fire behavior. For this reason, P1Early2, P1Early1, P1Delay1, and P1Delay2, as well as P6Early2, P6Early1, P6Delay1, and P6Delay2, were performed. Another way of examining the implications of using wind data from some distance away from the plot would be to use data from the other tower to derive the boundary conditions, but unfortunately those data are not available.

In 1997, when plot 6 was burned, wind data were collected once every 60 s. In 2000, when plot 1 was burned, wind data were collected once every 5 s. Thus, a second question that naturally arises concerns the impact of using high temporal resolution data to drive simulations and whether it is appropriate to average over 1-min intervals or even over the length of the burn. To address these questions, the P1Tavg1min, P1Tavg1minDelay2, P1Tavg, and P6Tavg simulations were performed, where the “T” in these names indicates time. P1Tavg1min is a simulation in which the 5 s data collected at tower 1 during the burning of plot 1 is averaged over 1-min intervals, which is similar to what was done with the wind data in 1997. P1Tavg1minDelay2 is averaged as for P1Tavg1min, but with the simulated ignition initiated 120 s late. P1Tavg and P6Tavg are simulations in which the wind

data are averaged over 6 min, which is nominally the length of time for the plot 1 and plot 6 burns.

Models such as FIRETEC can be used to investigate the potential coupled fire–atmosphere–vegetation impacts of artifacts such as the fuel breaks in the experimental design. In the P1Nobreaks and P6Nobreaks simulations, the fuel bed of the specified plot covers the entire  $400 \text{ m} \times 400 \text{ m}$  domain, so that the fuel breaks are computationally removed. Similarly, the fuel bed is expanded to cover the entire domain for P1NobreaksEarly1, P1NobreaksDelay1, P6NobreaksEarly1, and P6NobreaksDelay1, but the simulated ignitions were started 60 s early or 60 s late as described above.

## Results

The two most obvious ways to compare the results of the simulations described above are in terms of spread rates and burn patterns. For plot 1, the fire was ignited along the southern edge of the plot, with the igniter traveling from east to west. The maximum propagation distance was measured from the ignition line to the farthest northern location (farthest point forward in the  $y$  direction) where the solid temperature in the first level of computational cells above the ground was over 500 K. The spread rates reported in Stocks et al. (2004b) are also for ground fire propagation. The fire was ignited from east to west along the northern edge of plot 6, and the propagation distance in simulations is measured to the farthest southern point where solid temperatures were above 500 K.

**Table 1.** Summary of FIRETEC simulations in terms of relevant plot, wind data resolution and tower used for wind data acquisition, and time of ignition relative to the documented ignition time in the wind series,  $t_{\text{ign}(\text{rel})}$ , where  $t_{\text{ign}(\text{rel})} = t_{\text{ign}(\text{sim})} - t_{\text{ign}(\text{doc})}$ .

Simulation	Plot	Wind data resolution (tower number (1 or 2))	Relative ignition time (min)	Specifics
P1Base	1	5 s (1)	0	Ignition and wind series times are synchronized
P1Early2	1	5 s (1)	-2	
P1Early1	1	5 s (1)	-1	
P1Delay1	1	5 s (1)	+1	
P1Delay2	1	5 s (1)	+2	
P1Tavg1min	1	60 s (1)	0	5 s data averaged over 60 s periods
P1Tavg	1	5 s (1)	0	5 s data averaged over 6 min
P1Tavg1minDelay2	1	60 s (1)	+2	5 s data averaged over 60 s periods
P1NobreaksEarly1	1	5 s (1)	-1	Entire FIRETEC domain filled with plot 1 fuels
P1Nobreaks	1	5 s (1)	0	Entire FIRETEC domain filled with plot 1 fuels
P1NobreaksDelay1	1	5 s (1)	+1	Entire FIRETEC domain filled with plot 1 fuels
P6Base	6	60 s (2)	0	Ignition and wind series times are synchronized
P6Early2	6	60 s (2)	-2	
P6Early1	6	60 s (2)	-1	
P6Delay1	6	60 s (2)	+1	
P6Delay2	6	60 s (2)	+2	
P6Tavg	6	60 s (2)	0	60 s data averaged over 6 min
P6NobreaksEarly1	6	60 s (2)	-1	Entire FIRETEC domain filled with plot 6 fuels
P6Nobreaks	6	60 s (2)	0	Entire FIRETEC domain filled with plot 6 fuels
P6NobreaksDelay1	6	60 s (2)	+1	Entire FIRETEC domain filled with plot 6 fuels

**Table 2.** Average wind speeds are calculated over the duration of time that it takes for the fire to reach the far side of the burn plots.

Simulation	Average wind speed ( $\text{m}\cdot\text{s}^{-1}$ )	Average spread rate ( $\text{m}\cdot\text{s}^{-1}$ )
P1Base	2.8650	0.587
P1Early2	3.1522	0.648
P1Early1	3.0372	0.532
P1Delay1	2.9159	0.344
P1Delay2	3.0199	0.311
P1Tavg1min	2.8337	0.632
P1Tavg	2.9552	0.636
P1Tavg1minDelay2	2.9943	0.425
P1NobreaksEarly1	2.9736	0.566
P1Nobreaks	2.8518	0.576
P1NobreaksDelay1	2.9139	0.480
P6Base	4.3516	0.768
P6Early2	3.8977	0.666
P6Early1	4.0690	0.681
P6Delay1	4.1396	0.727
P6Delay2	3.9453	0.626
P6Tavg	4.0927	0.703
P6NobreaksEarly1	3.9268	0.625
P6Nobreaks	4.0094	0.607
P6NobreaksDelay1	3.7203	0.586

**Note:** Average spread rates are calculated over this same time period.

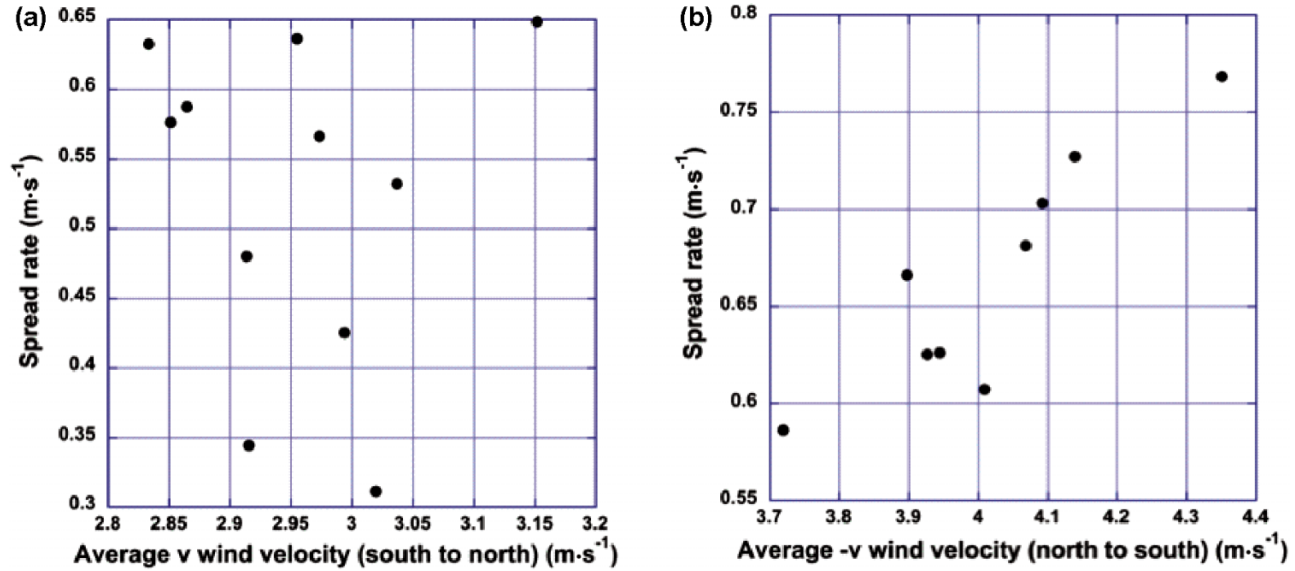
Linear curve fits to the propagation curves are used to determine the average spread rate for the fires in each simulation. Table 2 provides a summary of the average wind speed for the duration of each burn and the spread rate for the 20 simulations. Although the documented average spread rates for plots 1 and 6 from the experiments were  $0.588 \text{ m}\cdot\text{s}^{-1}$  and

$0.600 \text{ m}\cdot\text{s}^{-1}$ , respectively (Stocks et al. 2004b), which agrees well with the simulation results, the topic of most interest in this current work is the relative magnitudes of the simulated spread rates compared with each other. By comparing the spread rates of P1Base, P1Early2, P1Early1, P1Delay1, and P1Delay2, we see that the specific ignition time with respect to the phase of the fluctuating wind patterns does affect the net spread rate. Modifying the synchronization of the wind and fire ignition by 1 or 2 min early or late had 10%, -9%, -41%, and -47% effect on the spread rate under wind conditions that were not significantly globally increasing or decreasing over long periods of time (percentages for P1Early2, P1Early1, P1Delay1, and P1Delay2, where positive percentages indicate increases in spread rate over the base case).

Average wind speeds for the duration of each simulated burn period are provided in Table 2, and each fire's average spread rate is plotted against its average wind speed in Fig. 6. Table 2 and Fig. 6 illustrate that there are factors besides average wind speed that are contributing to the differences in the average spread rates of these simulated fires. Questions concerning the possible influence of factors such as gust frequency on spread rates could be posed.

To better understand the connections between the dynamic wind fields and fire spread rates, the propagation distances are shown in Figs. 7a, 7b, and 7c for the plot 1 simulations and in Figs. 7d and 7e for plot 6 simulations. Figures 7a and 7d illustrate the influence of shifting the ignition times by 1 or 2 min(s) earlier or later with respect to the winds for plots 1 and 6, respectively. Figures 7b and 7e illustrate the influences of fuel breaks on the spread for plots 1 and 6. Figure 7c illustrates the influence of temporal resolution of the wind fields in the simulations of plot 1. In these figures, the time axis measures relative to the documented ignition time of the

Fig. 6. Time-averaged spread rates as a function of time-averaged wind speeds during the various simulations for (a) plot 1 and (b) plot 6.



respective ICFME plot (16:01 for plot 1, 14:06 for plot 6; Stocks et al. 2004b).

In Fig. 7, propagation distances are described by the colored curves and the axis on the left of the plots. In Figs. 7a, 7b, and 7c, the magnitude of the winds from south to north ( $v$  component) is shown by the grey lines and the axis on the right of the plots. For Figs. 7d and 7e, the winds from north to south (negative  $v$  component) is shown by the grey lines and the axis on the right of the plots. By comparing the fire propagation of the various fire lines with the wind speeds in the direction of measured spread, the influence of accelerations or decelerations in the winds on the fire spread rate can be seen. As might be expected, in general, faster winds tend to be correlated with steeper sections of the propagation curves and thus faster spread rates, as the local slope of the colored curves is the instantaneous (or 1 s average, which is the frequency of the plotted data) spread rate of the fire.

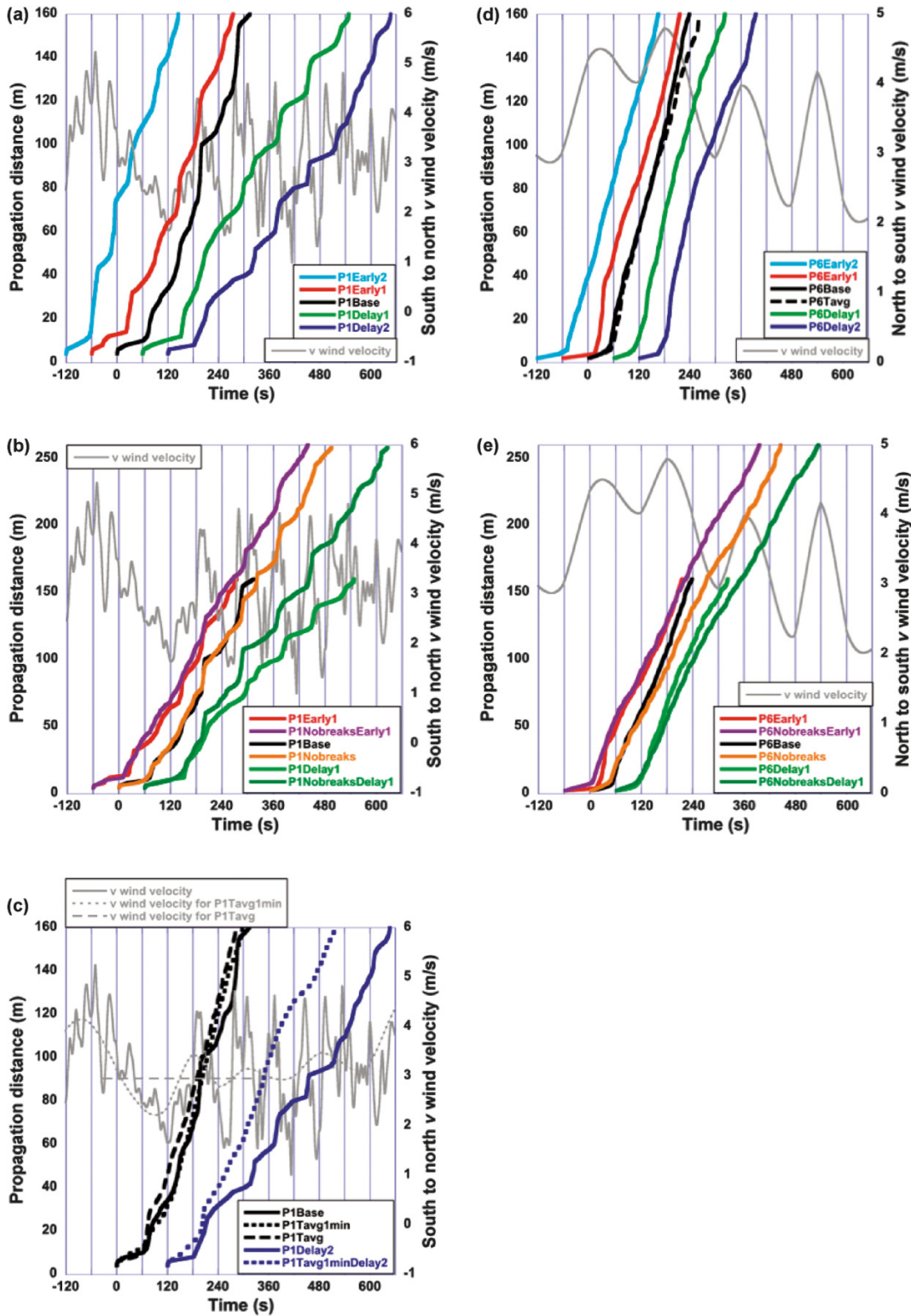
In each of the propagation curves in Fig. 7, an initial period of slow spread can be seen at the base of the curve. This period is related to the time period when the ignition is being drawn across the upwind side of the burn plot and the fire is establishing itself in the vegetation. In the simulations, it takes between 60 s and 100 s for the fires to begin picking up speed for all of the curves and seems to be somewhat affected by the magnitude of the velocity component during this time. It should be noted that the fire line is growing in length for the first 60 s as it takes the ignition vehicle this long to traverse the plot. After this ignition period, all of the simulated fires accelerate, but the overall speed of the resulting propagating fire depends on the details of the winds that drive them.

Comparing the fire propagation patterns with the wind fluctuations shows that there are periods when all of the simulated fires burning at a given time accelerate or decelerate in correlation with wind speed increases or decreases, as illustrated in Fig. 7a at 25 s, 200 s, and 375 s (accelerating) and 330 s and 470 s (decelerating). In other instances, the ac-

celerations or decelerations of various simulated fires are less consistent and show different degrees of response to shifts in the concurrent winds, e.g., at 45 s when P1Early2 is less affected by the decrease in wind speed than P1Early1, at 285 s when P1Base shows much larger acceleration than P1Delay1, or at 300 s when P1Delay1 accelerates and P1Delay2 nearly decelerates. This illustrates that in some cases when the wind changes, the duration of the change, as well as the specific fire configuration, history of the fire, and position of the fire on the plot, affects the fire's ability to react to the wind shifts. For example, more fully developed or faster moving fires may be less susceptible to lulls in the wind field or accelerate more slowly in the presence of a gust such as those seen at 45 s comparing P1Early2 and P1Early1 or at 270 s comparing P1Delay1 and P1Delay2.

Figure 7a includes the propagation from five simulations in which the only difference is the ignition time with respect to the wind field. One of the most obvious impacts of shifting the ignition time is seen in the P1Early2 curve, which illustrates a faster overall spread rate due to the fire's exposure to a set of sustained elevated velocities within 1 min after ignition. These velocities cause an early period of fast fire growth and intensification, which limits the impact of the initial portion of the velocity trough that hits a minimum around 125 s. P1Early1 and P1Base are both ignited during this lull in the  $v$ -component winds but then have the benefit of the steady rise in wind speed that peaks at nearly  $4.5 \text{ m}\cdot\text{s}^{-1}$  around 200 s. P1Delay1 and P1Delay2 are also exposed to peak winds of nearly  $4.5 \text{ m}\cdot\text{s}^{-1}$ , but these gusts occurring after 240 s oscillate with significant lulls with a higher frequency than the oscillations of gusts prior to 240 s. The lulls between wind gusts include a brief period when the winds drop to nearly  $1 \text{ m}\cdot\text{s}^{-1}$  at approximately 390 s, which in particular causes a significant reduction in spread rate and a delayed recovery. This anecdotally supports a preliminary hypothesis suggesting that the higher frequency gust patterns occurring after 200 s (on the order of 0.0167 Hz or one pe-

**Fig. 7.** Plots of propagation distance measured perpendicular to the ignition lines in FIRETEC simulations of ICFME plot fires: (a) plot 1 fires driven by 5 s wind data using various ignition times with respect to the wind time series; (b) plot 1 fires burning on landscapes with no fuel breaks using 5 s wind data; (c) plot 1 fires driven by averaged wind data using various ignition times with respect to the wind time series; (d) plot 6 fires driven by 60 s wind data using various ignition times with respect to the wind time series; and (e) plot 6 fires burning on landscapes with no fuel breaks using 60 s wind data. Grey lines show the interpolated  $v$  wind field in the direction of spread. Time series are measured relative to the documented ignition times.



riod every 60 s) result in reduced temporal continuity in spread and a net reduction in spread rate. This notion definitely requires further investigation through examination of field observations and subsequent numerical studies.

From the data provided in Table 2 and Figs. 6 and 7, similar analysis can be made for P6Base, P6Early2, P6Early1, P6Delay1, and P6Delay2. These plot 6 simulations also suggest that the particular time of ignition affects the overall spread rate of the fire, as 1 or 2 min early or late ignition caused  $-13\%$ ,  $-11\%$ ,  $-5\%$ , and  $-18\%$  differences in spread rates as compared with P6Base (percentages for P6Early2, P6Early1, P6Delay1, and P6Delay2, where positive percentages indicate increases in spread rate over the base case). However, with the exclusion of P6Delay2, the spread rates have smaller differences than between the various plot 1 simulations with early and delayed ignition times. Visual observation of the propagation curves in Fig. 7d reveals much less variation between the various fires' spread rates as they move across the burn plots than is seen in Fig. 7a, potentially due to the much more limited range of temporal frequencies of the variations in the plot 6 wind field data.

The implications of 0.2 Hz (5 s) vs. 0.0167 Hz (60 s) frequency wind data must be considered when analyzing the similarities and differences between the sensitivity of plot 1 and plot 6 to phase correlations between input winds and ignition times. This consideration also has ramifications connecting spread rates to wind speeds averaged over the duration of the burn. To gain more perspective on the sensitivity of the simulations to the frequency of the winds or the sampling rate of the data, P1Tavg1min, P1Tavg, and P1Tavg1minDelay2 were performed, and the propagation distances of these simulated fires are illustrated in Fig. 7c. P1Tavg1min and P1Tavg1minDelay2 used plot 1 wind data that were averaged over 1-min intervals, starting at the documented ignition time and 2 min late, respectively. P1Tavg used plot 1 wind data that were averaged over 6 min, starting at the documented ignition time. Average spread rates for these simulations are shown in Table 2.

Figure 7c includes propagation distance curves for P1Base, P1Tavg1min, and P1Tavg simulations, as well as P1Delay2 and P1Tavg1minDelay2 for comparison. By comparing the relatively small differences in P1Base and P1Tavg1min with the larger differences between P1Delay2 and P1Tavg1minDelay2, it is apparent that the impact of temporal averaging of the original 5 s data (0.2 Hz) over 1-min intervals (0.0167 Hz) is dependent on the specific time interval of the fires. In the 1-min average wind data, the  $\sim 0.015$  Hz ( $\sim 66$  s) oscillations that are seen in the 5 s wind data after 200 s disappear. The similarity between propagation curves P1Tavg1min and P1Tavg might suggest that for plot 1 fires, wind oscillations with time frequencies lower than 1 Hz do not have much impact on the spread rate. Consideration of the very different spread of the 2-min delay simulation to the 2-min delay with a 1-min filter (0.0167 Hz) data (P1Delay2 and P1Tavg1minDelay2, respectively) compared with the fairly similar P1Base and P1Tavg1min illustrates that the impact of filtering out the subminute fluctuations in the wind field is likely to be less when the ambient oscillations have dominant oscillation periods larger than a minute. Another way to consider this comparison is that there is less difference between the overall spread rates of the 1-min filtered wind

cases (P1Tavg1min and P1Tavg1minDelay2) than between respective simulations with unfiltered winds (P1Base and P1Delay2).

Likewise, Fig. 7c includes propagation curves for P1Tavg. The comparison of P1Tavg and P1Tavg1min with P1Base curves suggests that the impact of averaging winds to 1 min versus averaging over the duration of the fire is minimal with this wind field. However, this is not sufficient to conclude that averaging over 1 min or 6 min has no consequences. This practice should be considered with caution because this similarity could still be dependent on the importance of those fluctuations with time scales between 1 min and the length of the burn.

It is important to recognize that the size of the burn plots or the duration of the experiments plays a critical role in the variations in spread rates described above. More specifically, the size of the plots or duration of the experiments should be compared with the temporal scales of the wind fluctuations that are passing by the experiment. There are a number of fluctuations in the wind data that have time scales on the order of 1 to 3 min. It is important to consider the relative size of these fluctuations compared with the changes in simulated ignition time (0 to 2 min), as well as the length of time that it takes these fires to traverse the plots (3 to 5 min). The similar orders of magnitude of these time scales increases the sensitivity of the spread rate calculations to the timing of the ignition relative to the phase of the wind fluctuation for the following reasons: (i) a 1- or 2-min delay of the ignition has the potential for making significant shifts in the time of the ignition relative to the phase of the wind oscillations; and (ii) the duration of some of the most significant wind oscillations suggests that there is only time for a few of these oscillations during the course of an experiment. Therefore, there is an increase in the significance of correlations between various parts of the wind fluctuations and simultaneous fire geometries, amplifying the impact of the changing phase of the ignition. A larger experiment, or a shift in the frequency of the winds toward higher frequency fluctuations, might reduce the sensitivity of these average spread-rate calculations to the phase of the ignition relative to the wind fluctuations.

Figures 7b and 7e include propagation curves for simulations in which the fuel breaks for plots 1 and 6, respectively, have been removed from the simulation and the simulated fires are allowed to spread beyond the bounds of the experimental plots. The results from these simulations suggest several important concepts: (i) the presence of the fuel breaks could influence the spread rates within the bounds of the plot area; and (ii) the net influence of phase synchronization between wind and ignition is less when the fuel breaks are not present, presumably due to the differences in entrainment induced by the presence of the fuel breaks.

Although this is not an exhaustive set of simulations, or random, and is certainly not sufficient to generate a probability distribution, the variability of these results suggest several things, including the following: (i) the time of ignition relative to a particular time in the velocity patterns can be important for connecting overall spread rates to wind speeds in experiments; and (ii) if the specifics of the velocity fluctuations at the location of the fire are not known, there is a potential for significant uncertainty in any spread rate versus wind relationships derived from these experiments. Both the

frequency of the wind fluctuations during the experiment and the frequency of the data collection could have an impact on our ability to connect wind speed to spread rates definitively. An undocumented delay of ignition or imprecise synchronization of timing equipment begins to seem important for this scale of experiment. In addition, experimental designs that alter the fire's entrainment can potentially enhance (or potentially decrease) the sensitivity of the fire spread rates to the specifics of fluctuations in the wind.

Theoretically, it is easy enough to synchronize watches; however, an equally important concern is the implications of the spatial location of the wind towers relative to the fires. The issue that initially drove the need for these simulations was that the tower data were recorded at sites that were hundreds of metres from the experimental plots. Order-of-magnitude analysis suggests that if eddies in the wind field (those associated with the recorded fluctuations) are being transported at rates between  $2 \text{ m}\cdot\text{s}^{-1}$  and  $5 \text{ m}\cdot\text{s}^{-1}$  (it is impossible to define the precise actual transport velocity, but this order of magnitude is likely given the tower data), the time difference for a feature in the wind patterns to move 300 m is between 150 s and 60 s. If the flow patterns were moving from the plots towards the tower (ignoring the evolution of the flow pattern as it moved), then you would expect winds at the ignition site at the time of the ignition to be correlated with winds on the order of a minute or two later in the time series that was measured downwind at the tower. If the flow were to be moving from the tower to the plot, then you would expect the winds at the ignition site and ignition time to be correlated with points a minute or two earlier in the time series. As it is, the towers are not in line (upwind or downwind) with the simulated plots and are actually dislocated laterally as well. Therefore, the flow structures that are advected by the tower are not exactly the same as those carried over the plot. The time series of wind data is still useful in performing simulations because it suggests the correct nature of the fluctuations in the wind; however, it does not convey exactly where in the time series the ignition should start. Another consideration is whether the winds measured at the towers are being affected by the fire itself. If this happens, the wind data are much more difficult to use in specifying upwind conditions because somehow the fire's influence on the winds must be determined and filtered out. In this case, as mentioned above, the wind patterns do not suggest that the fire has a strong effect on the winds at the towers. The simulation domains do not include the location of the towers, but the extent of the fire-induced aspects of the wind patterns in the simulations suggests that the effects of fire entrainment as far away as the towers would be minimal.

Figures 8 and 9, showing fire perimeters for plot 1 at 300 s (Fig. 8) and plot 6 at 240 s (Fig. 9) after their respective ignitions, are included to illustrate the difference in fire perimeter geometry for the various simulations after the fires have propagated for this amount of time. These figures again illustrate that there are some differences in the downwind propagation, but there are also differences in the fire shape due to the lateral wind fluctuations and modification of the entrainment. These differences due to the interaction of lateral wind (or east–west component) fluctuations are most easily recognized by noticing the differences in location of the head of the fire in the crosswind direction. The propaga-

tion distances reported in Fig. 7 are slightly different than the perimeters indicated in Figs. 8, 9, 10, and 11 in that a 500 K temperature threshold was used to mark the forward progress in Fig. 7, whereas the demarcation of the black to grey in the other figures is based on the location where approximately one-third of the initial wet mass of the fuel is depleted. These two events do not occur at exactly the same time.

Figures 10 and 11 illustrate the burn patterns from the various plot 1 and plot 6 simulations without fuel breaks. Figure 10 includes images at 300 s and 480 s after ignition in the P1NobreaksEarly1 (Figs. 10a and 10b), P1Nobreaks (Figs. 10c and 10d), and P1NobreaksDelay1 (Figs. 10e and 10f). Likewise, Fig. 11 includes images at 240 s and 390 s after ignition in the P6NobreaksEarly1 (Figs. 11a and 11b), P6Nobreaks (Figs. 11c and 11d), and P6NobreaksDelay1 (Figs. 11e and 11f). In Figs. 10 and 11, the second image associated with each simulation depicts the influences of dynamic shifts in the crosswinds, or  $u$  component, of the wind field through the complex-shaped fire perimeters.

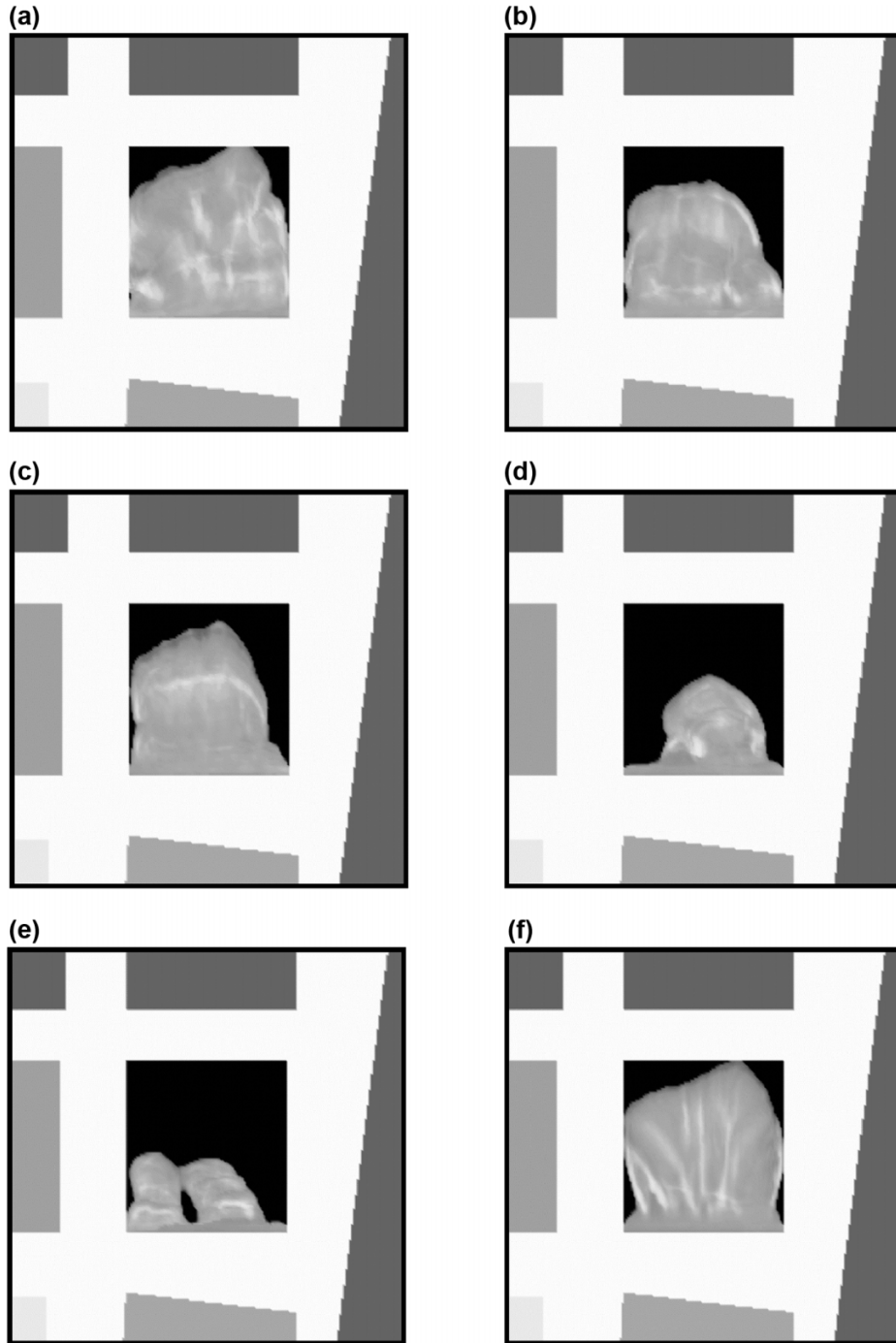
The images in Figs. 10a, 10c, and 10e can be compared with Figs. 8b, 8c, and 8d because the times are the same, 300 s, and ignitions were synchronized with the wind time series at the same times. Likewise, Figs. 11a, 11c, and 11e can be compared with Figs. 9b, 9c, and 9d, all of which are shown at 240 s after ignition. The comparison between the appropriate Fig. 10 and Fig. 8 plots shows that in the case of the 1 min early and base-time ignition, the downwind spread distances are comparable, as mentioned in the discussion of Fig. 7b. The comparison of the 1 min late cases also agrees with the discussion of Fig. 7b above in that the fire with no breaks has propagated farther at this point. This might suggest that the fuel breaks make the fire more susceptible to higher frequency gusts due to the reduction in resistance to entrainment. Another observation that can be made is that in the P1Early1 and P1Base simulations with fuel breaks, the fires appear to veer to the west, whereas the fires with no breaks do not show as much of this tendency. This difference could also be partially due to the changes in  $u$ -component wind penetration into the canopy in the cases with fuel breaks.

A comparison between the Fig. 11 and Fig. 9 images reveals that the differences in the fire behavior by 240 s between the simulations with and without fuel breaks is less noticeable for plot 6. This is true for both magnitude of spread and shape or direction of spread. It is worth noting that the crosswind fluctuations in the plot 6 wind field are even lower in frequency than the streamwise winds discussed before, whereas the plot 1 crosswind fluctuations have much higher frequencies than seen in plot 6.

## Conclusions

This work includes a series of FIRETEC simulations of ICFME plots 1 and 6. The selection of simulations for this manuscript centers around explorations of the implications of the variability in the wind field for model development, model validation, and interpretation of wind data. The simulations in this paper used horizontally homogeneous fuel beds for the various plots based on work published in previous literature. Careful attention was paid to the geometry of the plots and layout of the ICFME experimental site to

**Fig. 8.** Plot 1 simulations at 300 s: (a) P1Early2; (b) P1Early1; (c) P1Base; (d) P1Delay1; (e) P1Delay2; and (f) P1Tavg. The shades of grey indicate the density of fuel that is still present (black is maximum and white is minimum).



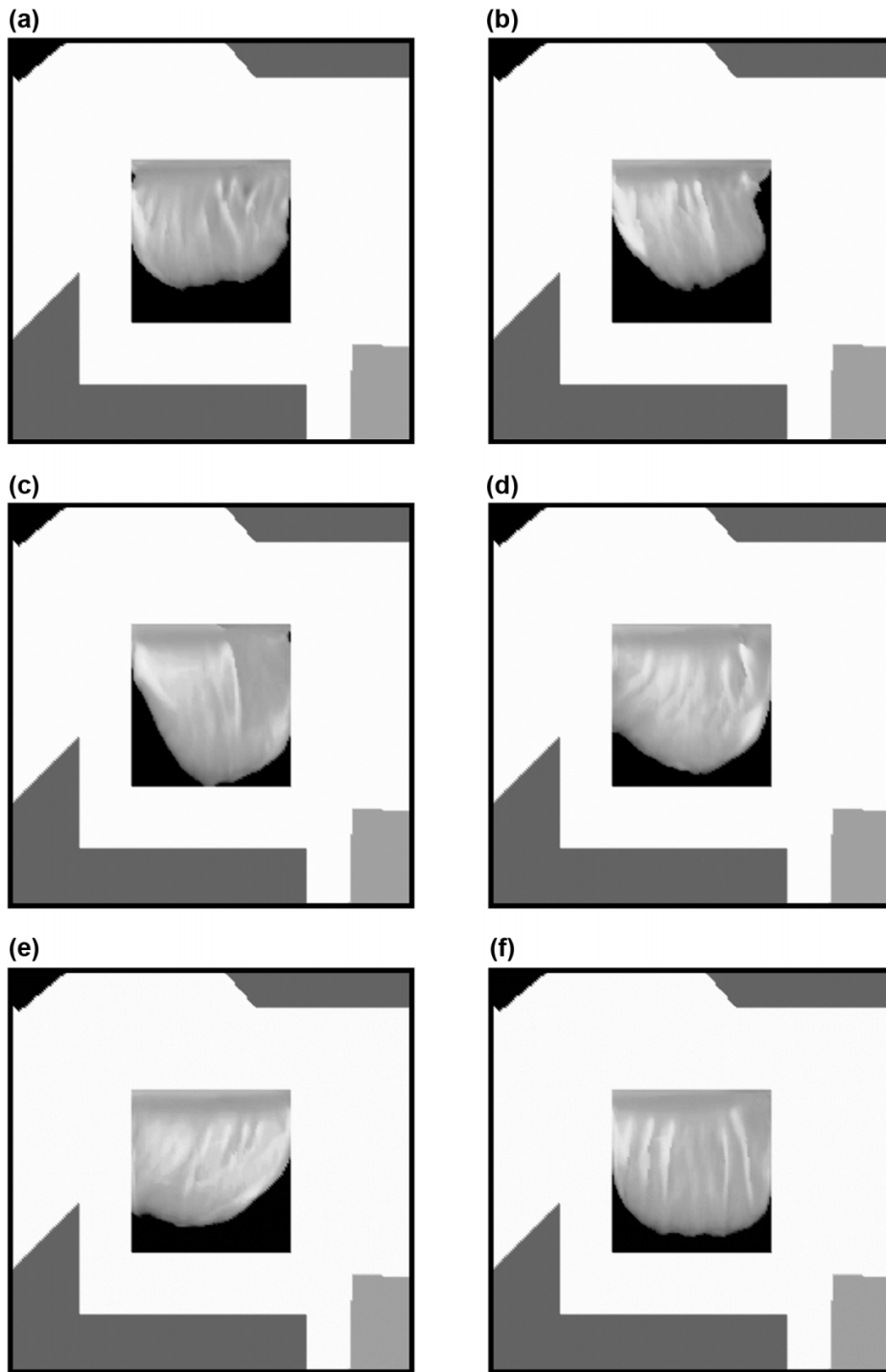
capture the impacts of the fuel breaks between the plots. Although this work focuses on aspects of using the measured wind data, parallel studies could also be pursued with respect to other aspects of fire experiments such as fuels data.

A description of results from simulations serving as preliminary explorations or illustrations of the possible sensitivity of wildland fire experiment results to wind-data collection and interpretation is included in this work. Although they are not exhaustive or universal descriptions of the sensitivity, they provide food for thought and consideration for future experimental and modeling work.

Simulations described in this text suggest that there is some sensitivity of fire behavior and average fire spread (averaged over the 150 m scales of the ICFME plots) to the timing of the fire ignition with respect to the wind fluctuations or gusts. In experimental fire scenarios or numerical fire simulations, it is important to understand the correlations between the timing of these events or, at a minimum, understand what uncertainties will result if the timing information is not available.

The results of the simulations suggest that for the scale of the ICFME plots, the specifics of the wind fluctuations and

**Fig. 9.** Plot 6 simulations at 240 s: (a) P6Early2; (b) P6Early1; (c) P6Base; (d) P6Delay1; (e) P6Delay2; and (f) P6Tavg. The shades of grey indicate the density of fuel that is still present (black is maximum and white is minimum).

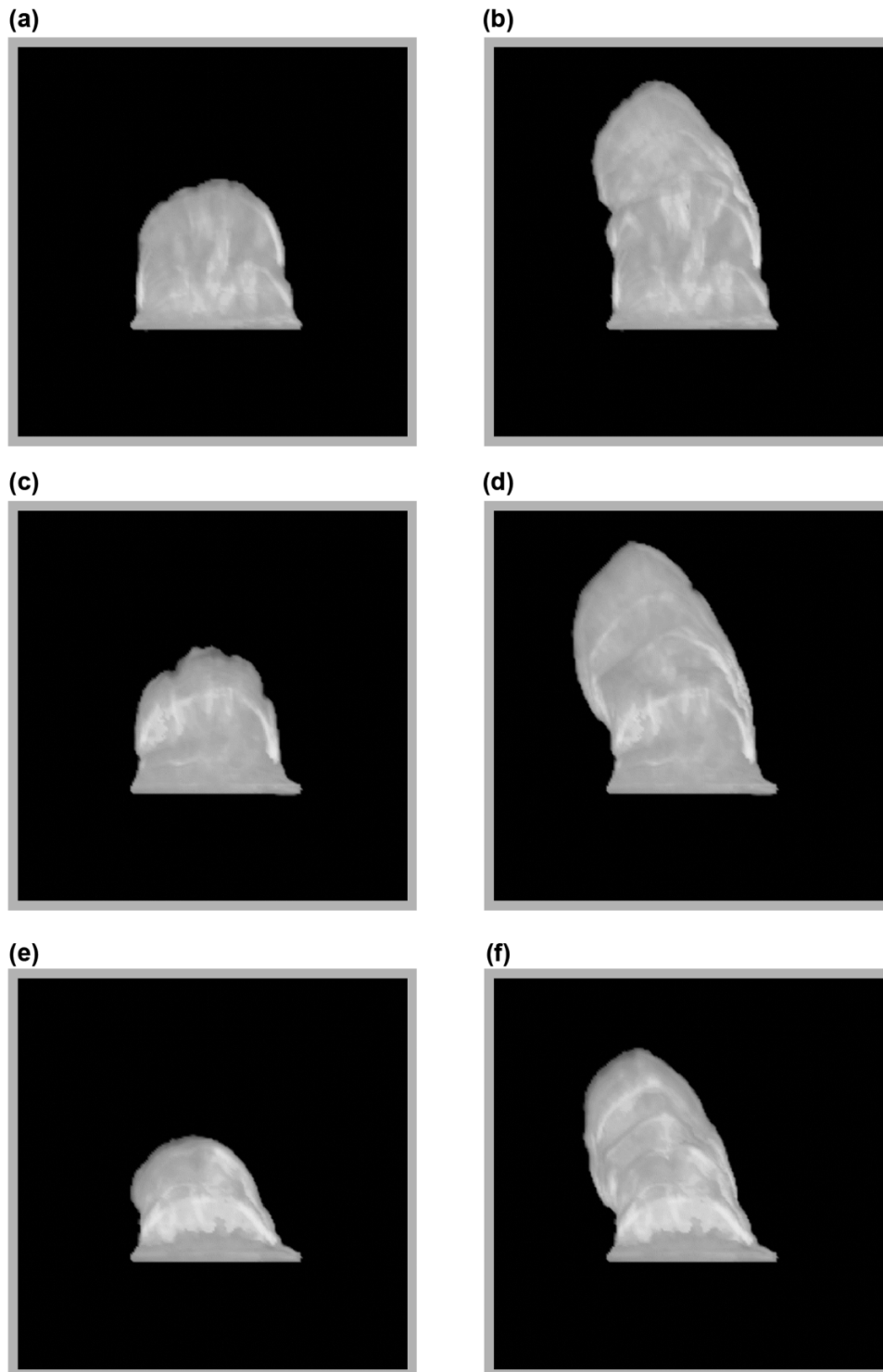


their phase relative to the ignition of the experiment can have noticeable effects on the average spread rates. The synchronization of specific wind fluctuations with fire events can lead to variations in average spread rate versus wind speed relationships and thus influence the parameters used to develop or validate models.

The rate at which wind data must be collected and recorded is not known; therefore simulations were performed with various levels of temporal averaging to gage the poten-

tial impacts of undersampling wind data. In the included simulations, averaging the wind data to 0.0167 Hz (60 s) affects fire-spread rates to varying degrees depending on the specific phase position of the ignition with respect to the wind fluctuations. The combined series of time-averaged simulations suggests that there are situations in which 1-min data lead to different simulation results than data taken at 5 s, and this is hypothesized to be related to the actual frequency of the winds.

**Fig. 10.** (a) P1NobreaksEarly1 at 300 s, (b) P1NobreaksEarly1 at 480 s, (c) P1Nobreaks at 300 s, (d) P1Nobreaks at 480 s, (e) P1NobreaksDelay1 at 300 s, and (f) P1NobreaksDelay1 at 480 s. The shades of grey indicate the density of fuel that is still present (black is maximum and white is minimum).

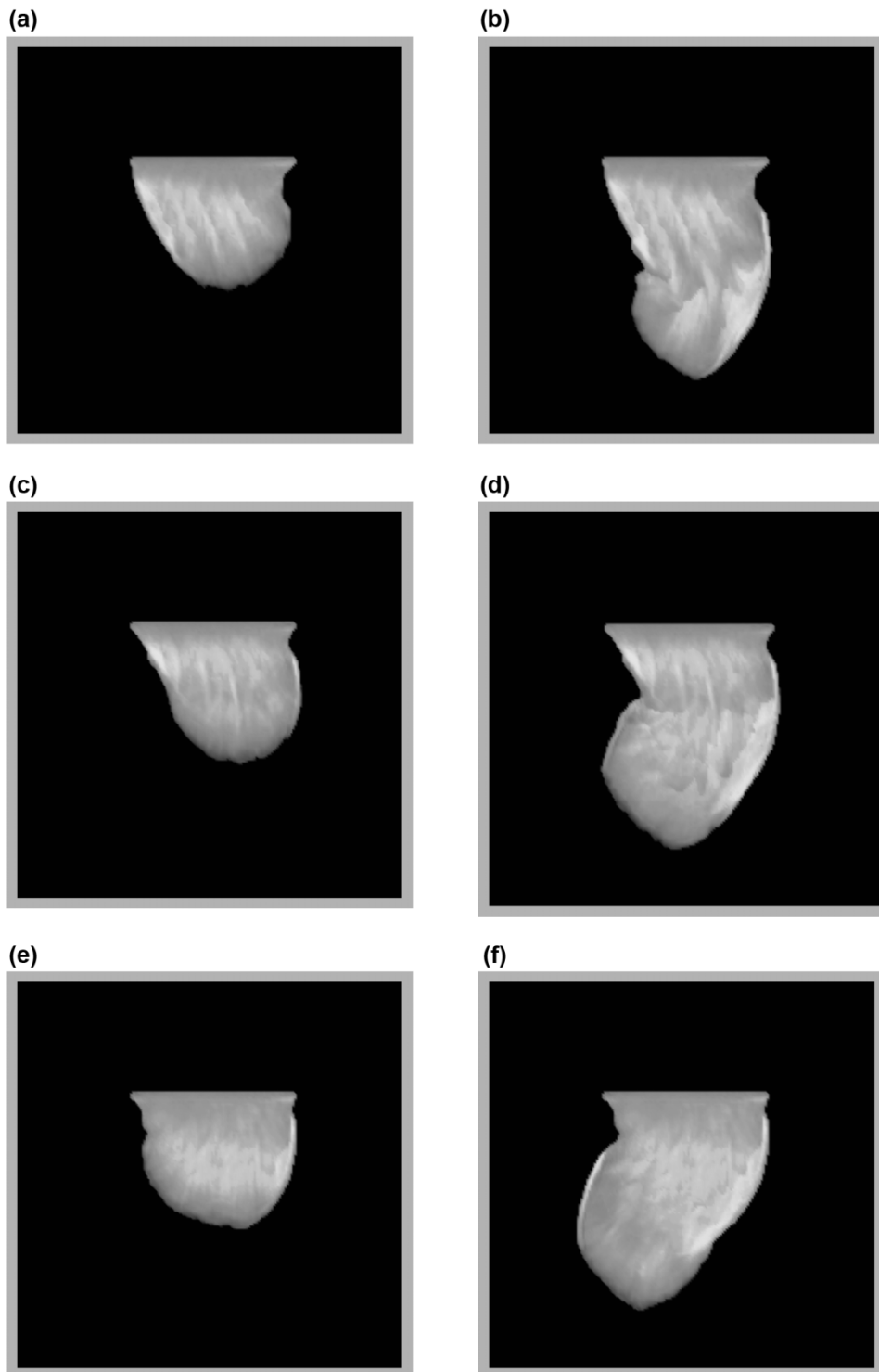


Simulations of fires in scenarios without fuel breaks were performed to sample possible implications of the experimental design on fire spread patterns and study impacts of the experimental design on the sensitivity of the simulated fires to wind fluctuations. As expected, the fuel breaks impacted the fire perimeter in both the downwind and lateral directions and had some influence on the spread rates in some wind

conditions. Interestingly, the presence of the fuel breaks seems to increase the fire spread rate's sensitivity to the details of the wind fluctuations.

In many experimental configurations, it is impractical to measure the wind immediately upwind of the burn plot. In some cases, such placement could result in the measurement of fire-influenced winds as opposed to ambient conditions.

**Fig. 11.** (a) P6NobreaksEarly1 at 240 s, (b) P6NobreaksEarly1 at 390 s, (c) P6Nobreaks at 240 s, (d) P6Nobreaks at 390 s, (e) P6NobreaksDelay1 at 240 s, and (f) P6NobreaksDelay1 at 390 s. The shades of grey indicate the density of fuel that is still present (black is maximum and white is minimum).



When wind data are collected at some significant distance away from the experimental plot (even 100s of metres), it is important to consider the implications of this displacement in terms of the wind data, in particular, wind fluctuations. The specific effects of the displacement between meteorological tower and the burn plot will be sensitive to the frequency of

the wind fluctuations, frequency of the wind data, and strength of the fluctuations. One way to understand the implications of such displacements is to consider the approximate size and transport speeds of the turbulent wind structures in comparison with the distance from the experimental plot, the size of the plot, and the duration over which the fires traverse

the plot. Multiple wind data collection sites could be used to obtain these quantities, but unfortunately, the wind towers along the sides of the burn plots could not be used for this purpose due to the fire's influence on the winds at their locations.

It is hypothesized that the size of the experimental plot or duration of the fire over which the data are collected also has implications for the required frequency of wind data. For short-duration tests, the implications for not knowing the specific phase of transient wind patterns can have a larger effect than for extended long-burning fires in which the specifics of the high frequency gusts are less important. The decline in the impact of the correlation of ignition time and short-duration gusts is related to the decline in the ratio between the period of perturbations in the wind time series and the length of time for the fires to burn (in other words, the increase in the number of fluctuations occurring during the burning period).

Through the consideration of some of these issues at the inception of an experiment, it might be possible to enhance the value of the data. On the other hand, wildland fire experiments are very costly, complicated, and quite messy by nature. Ideally, measurements would be taken on free-burning fires; however, limitations on preburn sampling, weather instrumentation, and safety issues make such observations very difficult. The cost of experimental campaigns such as ICFME, concerns over environmental impacts (both on the site and downwind), and safety constraints are likely to continue to limit the frequency of such extensive fire measurement opportunities. There will always be imperfections, assumptions, approximations, and missing data at some scale in these types of experiments. Thus, it is equally or more important that model developers and model validators consider the implications of the data-collection methods. It is critical to understand the assumptions and uncertainties that are inherent when incorporating experimental data in analysis and modeling contexts.

The focus of this work is not on the accuracy of the specific FIRETEC results as compared with experimental data, but on the sensitivity of the simulation results to aspects of wind data collection and the implications for interpretation, which might otherwise be ignored or at least considered insignificant. The most significant outcome of this work is to hopefully incite further discussion regarding design for future wildfire experiments and the appropriate applications, assumptions, and caveats for the use of experimental data for validation or calibration of models.

## Acknowledgements

The Los Alamos National Laboratory Institutional Computing Program provided critical computing resources for this work. Financial support for this work was provided by the National Fire Plan through the USDA Forest Service Washington Office and Rocky Mountain Research Station. Marty Alexander provided considerable assistance in reviewing the data collected for the ICFME experiments and answering questions concerning its interpretation. Jim Gould also provided insight and additional perspective through detailed discussions concerning some of the ICFME FIRETEC model results.

## References

- Alexander, M.E., Steffner, C.N., Mason, J.A., Stocks, B.J., Hartley, G.R., Maffey, M.E., Wotton, B.M., Taylor, S.W., Lavoie, N., and Dalrymple, G.N. 2004. Characterizing the jack pine – black spruce fuel complex of the International Crown Fire Modelling Experiment (ICFME). Canadian Forest Service Northern Forestry Centre Information Report NOR-X-393.
- Butler, B.W., Cohen, J., Latham, D.J., Schuette, R.D., Sopko, P., Shannon, K.S., Jimenez, D., and Bradshaw, L.S. 2004a. Measurements of radiant emissive power and temperatures in crown fires. *Can. J. For. Res.* **34**(8): 1577–1587. doi:10.1139/x04-060.
- Butler, B.W., Finney, M.A., Andrews, P.L., and Albini, F.A. 2004b. A radiation-driven model for crown fire spread. *Can. J. For. Res.* **34**(8): 1588–1599. doi:10.1139/x04-074.
- Clark, T.L., Jenkins, M.A., Coen, J., and Packham, D. 1996. A coupled atmosphere–fire model: convective feedback on fire-line dynamics. *J. Appl. Meteorol.* **35**(6): 875–901. doi:10.1175/1520-0450(1996)035<0875:ACAMCF>2.0.CO;2.
- Clark, T.L., Radke, L., Coen, J., and Middleton, D. 1999. Analysis of small scale convective dynamics in a crown fire using infrared video camera imagery. *J. Appl. Meteorol.* **38**(10): 1401–1420. doi:10.1175/1520-0450(1999)038<1401:AOSSCD>2.0.CO;2.
- Cohen, J.D. 2004. Relating flame radiation to home ignition using modeling and experimental crown fires. *Can. J. For. Res.* **34**(8): 1616–1626. doi:10.1139/x04-049.
- Cruz, M.G., Alexander, M.E., and Wakimoto, R.H. 2003. Assessing the probability of crown fire initiation based on fire danger indices. *For. Chron.* **79**(5): 976–983.
- Cruz, M.G., Alexander, M.E., and Wakimoto, R.H. 2004. Modeling the likelihood of crown fire occurrence in conifer forest stands. *For. Sci.* **50**(5): 640–658.
- de Groot, W.J., Bothwell, P.M., Taylor, S.W., Wotton, B.M., Stocks, B.J., and Alexander, M.E. 2004. Jack pine regeneration and crown fires. *Can. J. For. Res.* **34**(8): 1634–1641. doi:10.1139/x04-073.
- Linn, R.R. 1997. A transport model for prediction of wildfire behavior. Los Alamos National Laboratory Report LA-13334-T.
- Linn, R., Reisner, J., Colman, J.J., and Winterkamp, J. 2002. Studying wildfire behavior using FIRETEC. *Int. J. Wildland Fire*, **11**(4): 233–246. doi:10.1071/WF02007.
- Linn, R., Canfield, J., Winterkamp, J., Cunningham, P., Colman, J.J., Edminster, C., and Goddrick, S.L. 2005a. Numerical simulations of fires similar to the International Crown Fire Modeling Experiment. *In Proceedings 6th Fire and Forest Meteorology Symposium and 19th Interior West Fire Council Meeting, Canmore, Alberta, Canada, 24–27 October 2005.* Available from <http://ams.confex.com/ams/6FireJoint/techprogram/MEETING.HTM>.
- Linn, R., Winterkamp, J., Colman, J.J., Edminster, C., and Bailey, J.D. 2005b. Modeling interactions between fire and atmosphere in discrete element fuel beds. *Int. J. Wildland Fire*, **14**(1): 37–48. doi:10.1071/WF04043.
- Lynch, J.A., Clark, J.S., and Stocks, B.J. 2004. Charcoal production, dispersal, and deposition from the Fort Providence experimental fire: interpreting fire regimes from charcoal records in boreal forests. *Can. J. For. Res.* **34**(8): 1642–1656. doi:10.1139/x04-071.
- Mell, W., Jenkins, M.A., Gould, J., and Cheney, P. 2007. A physics-based approach to modelling grassland fires. *Int. J. Wildland Fire*, **16**(1): 1–22. doi:10.1071/WF06002.
- Payne, N.J., Stocks, B.J., Robinson, A., Wasey, M., and Strapp, J.W. 2004. Combustion aerosol from experimental crown fires in a boreal forest jack pine stand. *Can. J. For. Res.* **34**(8): 1627–1633. doi:10.1139/x04-052.
- Peterson, E.W., and Hennessey, J.P., Jr. 1978. Use of power laws for

- estimates of wind power potential. *J. Appl. Meteorol.* **17**(3): 390–394. doi:10.1175/1520-0450(1978)017<0390:OTUOPL>2.0.CO;2.
- Pimont, F., Dupuy, J.-L., Linn, R.R., and Dupont, S. 2009. Validation of FIRETEC wind-flows over a canopy and a fuel-break. *Int. J. Wildland Fire*, **18**(7): 775–790. doi:10.1071/WF07130.
- Plate, E.J. 1971. Aerodynamic characteristics of atmospheric boundary layers. U.S. Atomic Energy Commission, Division of Technical Information; available from National Technical Information Service, U.S. Department of Commerce, Springfield, Virginia.
- Putnam, T., and Butler, B.W. 2004. Evaluating fire shelter performance in experimental crown fires. *Can. J. For. Res.* **34**(8): 1600–1615. doi:10.1139/x04-091.
- Reisner, J., Wynne, S., Margolin, L., and Linn, R. 2000. Coupled atmospheric-fire modeling employing the method of averages. *Mon. Weather Rev.* **128**(10): 3683–3691. doi:10.1175/1520-0493(2001)129<3683:CAFMET>2.0.CO;2.
- Stocks, B.J., Alexander, M.E., and Lanoville, R.A. 2004a. Overview of the International Crown Fire Modelling Experiment (ICFME). *Can. J. For. Res.* **34**(8): 1543–1547. doi:10.1139/x04-905.
- Stocks, B.J., Alexander, M.E., Wotton, B.M., Stefner, C.N., Flannigan, M.D., Taylor, S.W., Lavoie, N., Mason, J.A., Hartley, G.R., Maffey, M.E., Dalrymple, G.N., Blake, T.W., Cruz, M.G., and Lanoville, R.A. 2004b. Crown fire behaviour in a northern jack pine – black spruce forest. *Can. J. For. Res.* **34**(8): 1548–1560. doi:10.1139/x04-054.
- Taylor, S.W., Wotton, B.M., Alexander, M.E., and Dalrymple, G.N. 2004. Variation in wind and crown fire behaviour in a northern jack pine – black spruce forest. *Can. J. For. Res.* **34**(8): 1561–1576. doi:10.1139/x04-116.